How do polymer molecular weights influence luminescence properties of metal-containing polymers?

A case study of platinum(II) complex end-functionalized polymers

Qun He,[a] Chen Wang,[a] Jie Xiao,[a] Yongyue Wang,[a] Yufeng Zhou,[b] Nan Zheng,[c] Bin Zhang*[b] and Weifeng Bu*[a]

[a]Key Laboratory of Nonferrous Metals Chemistry and Resources Utilization of Gansu Province, State Key Laboratory of Applied Organic Chemistry, and College of Chemistry and Chemical Engineering, Lanzhou University, Lanzhou, 730000, China

[b]School of Materials Science & Engineering, Zhengzhou University, Zhengzhou, 450002, China

[c]State Key Laboratory of Luminescent Materials and Devices, South China University of Technology, Guangzhou, 510640, China

*E-mail: binzhang@zzu.edu.cn
*E-mail: buwf@lzu.edu.cn

EXPERIMENTAL SECTION

General Considerations. Methoxypolyethylene glycol (**MePEG$_{45}$**, **MePEG$_{113}$**, **MePEG$_{226}$**, and **MePEG$_{454}$**) were purchased from *Sigma-Aldrich*. Polyethylene glycol (**PEG$_{45}$**, **PEG$_{72}$**, and **MePEG$_{118}$**) were purchased from *TCI*. 2,6-Bis(*N*-methylbenzimidazol-2'-yl)-4-hydroxypyridine (**L**) was prepared according to the procedure described in the literature.[S1] All of the PEG reagents were freeze-dried for 12 h before use to remove traces of water. Other chemicals were commercially used without further purification.

^{1}H and ^{13}C NMR spectra were carried out with a *JNM-ESC400* spectrometer, during which the samples were dissolved in *d*-chloroform (CDCl$_3$). Chemical shifts are noted in ppm and coupling constants in Hz. ^{1}H NMR spectra were calibrated according to the residual solvent peak (C*H*Cl$_3$ δ = 7.26 ppm). ^{13}C NMR spectra were calibrated according to the solvent peak (*C*DCl$_3$, δ = 77.16 ppm). Gel permeation chromatography (GPC) plots were recorded on a Shimadzu LC-20AD instrument with a calibration standard of polyethylene glycol and an eluent solvent of tetrahydrofuran (THF). The flow rate was 1.0 mL min^{-1} and the column temperature was kept at 40 °C. C, H, and N elemental analyses were obtained with Elementar Analysensysteme GmbH VarioEL elemental analyzer (Germany). Small-angle X-ray scattering (SAXS) and wide-angle X-ray scattering (WAXS) measurements were simultaneously carried out on a Nano-inXider (λ = 0.154 nm, Xenocs, France). During the experimental process, the X-ray source was a 40-μm-microfocus sealed tube with a copper anode and the total power was 30 W. Emission spectra, quantum yields, and luminescence lifetimes were measured using an Edinburgh Instruments FLS920 fluorescence spectrometer. The quantum yields were obtained according to an absolute method by utilizing an integrating sphere (150 mm diameter, PTFE coating), during which a 450 W Xe arc lamp was used as the steady-state excitation source. For lifetime measurements, a supercontinuum laser was used as the excitation source.

Synthetic Procedures and Characterization Details.

MePEG$_{45}$-Ms:[S2] Methoxypolyethylene glycol (**MePEG$_{45}$**, 2.01 g, 1mmol, 1 eq.) was dissolved in dry CH_2Cl_2 (50 mL), and freshly distilled triethylamine (0.69 mL, 5 mmol, 5 eq.) was added. The mixture was cooled at 0 °C and methanesulfonylchloride (0.39 mL, 5 mmol, 5 eq.) was added dropwise with vigorous stirring over 30 min. The reaction mixture was allowed to warm to room temperature and stirred for another 24 h. During this period, the reaction mixture slowly turned yellowish and some solids precipitated out. After removing the solid by filtration, the reaction mixture was washed three times with saturated $NaHCO_3$ solution. After drying over anhydrous $MgSO_4$, the organic layer was concentrated under reduced pressure and precipitated by addition of cold diethyl ether. The product was obtained as a white solid by filtration and dried under vacuum with a yield of 97% (2.03 g). ^1H NMR (400 MHz, CDCl$_3$): δ 4.38 (t, J = 4.4 Hz, 2H, MsOCH_2-), 3.76 (t, J = 4.4 Hz, 2H, MsOCH$_2$CH_2-), 3.72-3.45 (176H, polyethylene glycol peak), 3.38 (s, 3H, CH_3O-PEG), 3.09 (s, 3H, CH_3SO$_3$-) (Figure S1).

MePEG$_{113}$-Ms, **MePEG$_{226}$-Ms**, **MePEG$_{454}$-Ms**, **PEG$_{45}$-Ms$_2$** (Figure S2), **PEG$_{72}$-Ms$_2$**, and **PEG$_{188}$-Ms$_2$** were synthesized in an analogous procedure described for **MePEG$_{45}$-Ms**, but using **MePEG$_{113}$**, **MePEG$_{227}$**, **MePEG$_{454}$**, **PEG$_{45}$**, **PEG$_{72}$**, and **PEG$_{188}$** as reactants, respectively. The isolated yields were equal to or larger than 95% on the basis of the corresponding MePEG$_n$ precursors.

MePEG$_{45}$-L: 2,6-Bis(*N*-methylbenzimidazol-2'-yl)-4-hydroxypyridine (**L**, 0.50 g, 1.4 mmol, 1.4 eq.) was stirred with anhydrous powdered K$_2$CO$_3$ (0.59 g, 4.27 mmol, 4.3 eq.) in 2-butanone (30 mL) at 80 °C for 30 min. Then, **MePEG$_{45}$-Ms** (2.09 g, 1.0 mmol, 1 eq.) and KI (0.17 g, 1.0 mmol, 1 eq.) were added. The reaction mixture was kept at 80 °C for 48 h before removal of the solvent in vacuo. The residue was dispersed in CH$_2$Cl$_2$ and the undissolved solid was removed by filtration through Celite. The filtrate was washed three times with saturated NaCl solution. The organic layer was dried over anhydrous MgSO$_4$ and evaporated under reduced pressure. The product was further purified by precipitation of the CH$_2$Cl$_2$ solution in cold diethyl ether twice, and the product was obtained with a yield of 100% (2.35 g). ^1H NMR (400 MHz, CDCl$_3$): δ 7.96 (s, 2H), 7.86 (dd, J = 7.1, 1.3 Hz, 2H), 7.46 (dd, J = 7.2, 1.2 Hz, 2H), 7.40-7.33 (m, 4H), 4.41 (t, J = 4.6 Hz, 2H), 4.24 (s, 6H), 3.93 (t, J = 4.6 Hz, 2H), 3.83-3.45 (polyethylene glycol peak, 176H), 3.38 (s, 3H). ^{13}C NMR (CDCl$_3$, 100 M Hz): δ 166.06, 151.28, 150.23, 142.57, 137.32, 123.54, 122.54, 120.08, 111.90, 110.09, 71.75, 70.97, 70.51, 69.50, 68.00, 58.93, 32.11 (Figure S3). GPC: M_n = 2100, PDI = 1.03; $M_{n, NMR}$ = 2352 (Table S1).

MePEG$_{113}$-L: **MePEG$_{113}$-L** was synthesized following the procedure described for **MePEG$_{45}$-L**, but using **MePEG$_{113}$-Ms** (2.04 g, 0.4 mmol) as the reactant precursor. Yield: 2.06 g (96%). ^1H NMR (400 MHz, CDCl$_3$): δ 7.95 (s, 2H), 7.85 (dd, J = 6.8, 1.5 Hz, 2H), 7.45 (dd, J = 7.0, 1.2 Hz, 2H), 7.40-7.36 (m, 4H), 4.40 (t, J = 4.5 Hz, 2H), 4.24 (s, 6H), 3.93 (t, J = 4.5 Hz, 2H), 3.82-3.44 (polyethylene glycol peak, 448H), 3.37 (s, 3H). ^{13}C NMR (CDCl$_3$, 100 M Hz): δ 166.27, 151.11, 150.23, 142.43, 137.14, 123.53, 122.78, 120.08, 111.77, 109.93, 71.88, 70.97, 70.52, 69.21, 68.20, 59.00, 32.52 (Figure S4). GPC: M_n = 5100, PDI = 1.03; $M_{n, NMR}$ = 5347 (Table S1).

MePEG$_{226}$-L: **MePEG$_{226}$-L** was synthesized following the procedure described for **MePEG$_{45}$-L**, but using **MePEG$_{227}$-Ms** (2.01 g, 0.2 mmol) as the reactant precursor. Yield: 1.96 g (95%). ^1H NMR (400 MHz, CDCl$_3$): δ 7.94 (s, 2H), 7.84 (d, J = 7.1 Hz, 2H), 7.44 (d, J = 7.5 Hz, 2H), 7.38-7.31 (m, 4H), 4.39 (t, J = 4.1 Hz, 2H), 4.22 (s, 6H), 3.91 (t, J = 4.0 Hz, 2H), 3.79-3.43 (polyethylene glycol peak, 900H), 3.36 (s, 3H) (Figure S5). GPC: M_n = 9200, PDI = 1.04; $M_{n, NMR}$ = 10325 (Table S1).

MePEG454-L: **MePEG454-L** was synthesized following the procedure described for **MePEG45-L**, but using **MePEG454-Ms** (2.01 g, 0.1 mmol) as the reactant precursor. Yield: 1.94 g (95%).^{1}H NMR (400 MHz, CDCl$_3$): δ 7.95 (s, 2H), 7.86 (dd, J = 7.0, 1.6 Hz, 2H), 7.46 (dd, J = 7.3, 1.2 Hz, 2H), 7.41-7.32 (m, 4H), 4.40 (t, J = 4.6 Hz, 2H), 4.24 (s, 6H), 3.93 (t, J = 4.6 Hz, 2H), 3.82-3.45 (polyethylene glycol peak, 1812H), 3.37 (s, 3H) (Figure S6). GPC: M_n = 21900, PDI = 1.06; $M_{n, NMR}$ = 20369 (Table S1).

PEG45-L2 was synthesized following the procedure described for **MePEG45-L**, but using **L** (0.94 g, 2.64 mmol, 2.8 eq.) and **PEG45-Ms2** (2.03 g, 0.94 mmol, 1 eq.) as the reactant precursors. Yield: 2.49 g (99%). ^{1}H NMR (400 MHz, CDCl$_3$): δ 7.96 (s, 4H), 7.86 (dd, J = 6.8, 1.5 Hz, 4H), 7.47 (dd, J = 7.0, 1.7 Hz, 4H), 7.41-7.33 (m, 8H), 4.41 (t, J = 4.6 Hz, 4H), 4.24 (s, 12H), 3.94 (t, J = 4.6 Hz, 4H), 3.84-3.45 (polyethylene glycol peak, 172H). ^{13}C NMR (CDCl$_3$, 100 M Hz): δ 166.20, 151.04, 150.15, 142.35, 137.08, 123.48, 122.73, 120.01, 111.71, 109.89, 70.90, 70.45, 69.15, 68.14, 32.47 (Figure S7). GPC: M_n = 2400, PDI = 1.02; $M_{n, NMR}$ = 2675 (Table S1).

PEG72-L2 was synthesized following the procedure described for **MePEG45-L**, but using **L** (0.60 g, 1.69 mmol, 2.8 eq.) and **PEG72-Ms2** (2.01 g, 0.60 mmol, 1 eq.) as the reactant precursors. Yield: 2.15 g (93%). ^{1}H NMR (400 MHz, CDCl$_3$): δ 7.96 (s, 4H), 7.86 (dd, J = 6.6, 1.3 Hz, 4H), 7.46 (dd, J = 7.1, 1.8 Hz, 4H), 7.42-7.32 (m, 8H), 4.41 (t, J = 4.4 Hz, 4H), 4.24 (s, 12H), 3.93 (t, J = 4.4 Hz, 4H), 3.82-3.45 (polyethylene glycol peak, 280H). ^{13}C NMR (CDCl$_3$, 100 M Hz): δ 166.00, 150.89, 149.95, 142.20, 136.92, 123.31, 122.54, 119.81, 111.51, 109.76, 70.37, 70.28, 68.98, 67.96, 32.32 (Figure S8). GPC: M_n = 3200, PDI = 1.02; $M_{n, NMR}$ = 3864 (Table S1).

PEG188-L2 was synthesized following the procedure described for **MePEG45-L**, but using **L** (0.24 g, 0.68 mmol, 2.8 eq.) and **PEG188-Ms2** (2.00 g, 0.24 mmol, 1 eq.) as the reactant precursors. Yield: 2.05 g (97%). ^{1}H NMR (400 MHz, CDCl$_3$): δ 7.96 (s, 4H), 7.86 (dd, J = 6.8, 1.1 Hz, 4H), 7.46 (dd, J = 7.6, 1.2 Hz, 4H), 7.40-7.33 (m, 8H), 4.40 (t, J = 4.4 Hz, 4H), 4.24 (s, 12H), 3.93 (t, J = 4.6 Hz, 4H), 3.82-3.44 (polyethylene glycol peak, 744H). ^{13}C NMR (CDCl$_3$, 100 M Hz): δ 165.88, 150.62, 149.64, 141.81, 136.71, 123.26, 122.50, 119.57, 111.49, 109.70, 70.58, 70.16, 68.84, 67.88, 32.24 (Figure S9). GPC: M_n = 9000, PDI = 1.04; $M_{n, NMR}$ = 8975 (Table S1).

MePEG45-Pt: K$_2$PtCl$_4$ (0.20 g, 0.48 mmol) was added to a solution of **MePEG_45-L** (1.00 g, 0.43 mmol) in DMSO/CHCl$_3$ (15 mL/5 mL). The reaction mixture was kept at 90 °C for 7 days. After removal of the solvents under reduced pressure, the residue was dispersed in water and dialyzed successively against 0.1 mol L^{-1} NaCl solution and water. The dialyzed solution was subsequently filtered through celite and the filtrate was freeze-dried to give an orange solid. Yield: 1.07 g (96%).

MePEG113-Pt, **MePEG227-Pt**, **MePEG454-Pt**, **PEG45-Pt2**, **PEG72-Pt2**, and **PEG188-Pt2** were synthesized in an analogous procedure described for **MePEG45-Pt**, but using **MePEG113-L**, **MePEG227-L**, **MePEG454-L**, **PEG45-L2**, **PEG72-L2**, and **PEG188-L2** as reactant ligands, respectively. The isolated yields were equal to or larger than 95% on the basis of the corresponding **MePEG$_n$-L** or **PEG$_n$-L2** precursors.

These platinum(II)-containing polymers were further subjected to the measurements of elemental analyses. The results indicated that the ligands of **MePEG$_n$-L** and **PEG$_n$-L2** was completely coordinated to form the platinum(II)-containing polymers of **MePEG$_n$-Pt** and **PEG$_n$-Pt2**, respectively (Table S2).
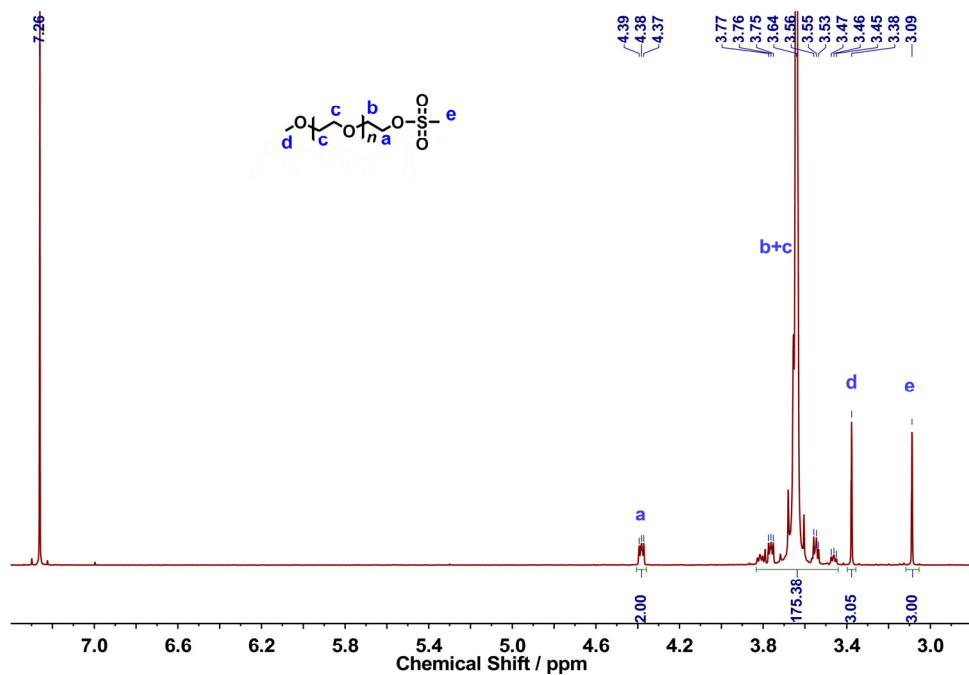
Fig. S1 ^{1}H spectra of **MePEG$_{45}$-Ms** in CDCl$_3$.
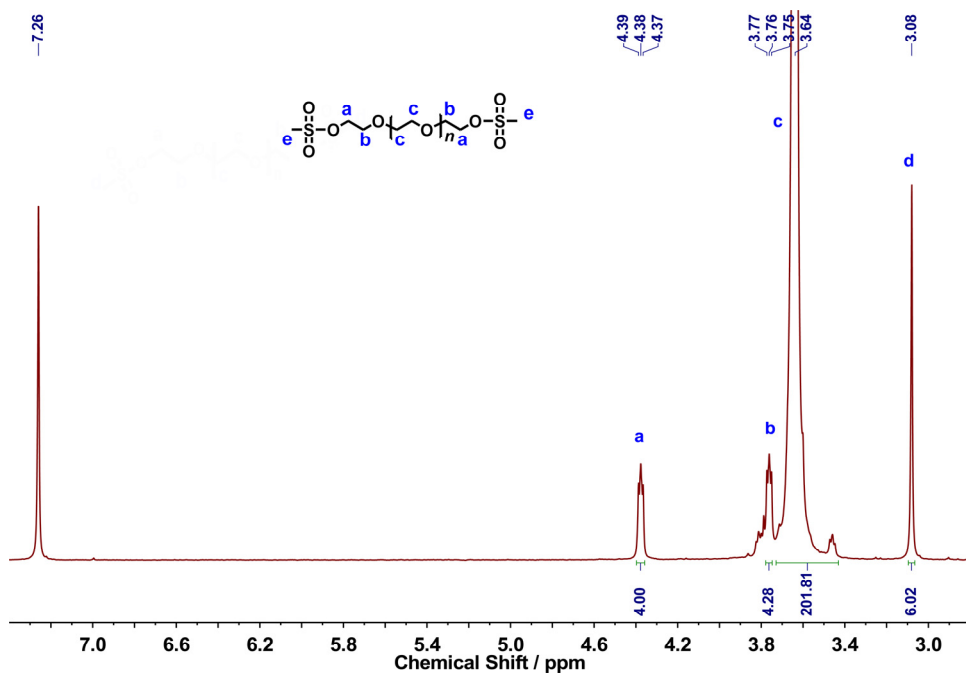
Fig. S2 ^{1}H spectra of **PEG$_{45}$-Ms$_2$** in CDCl$_3$.
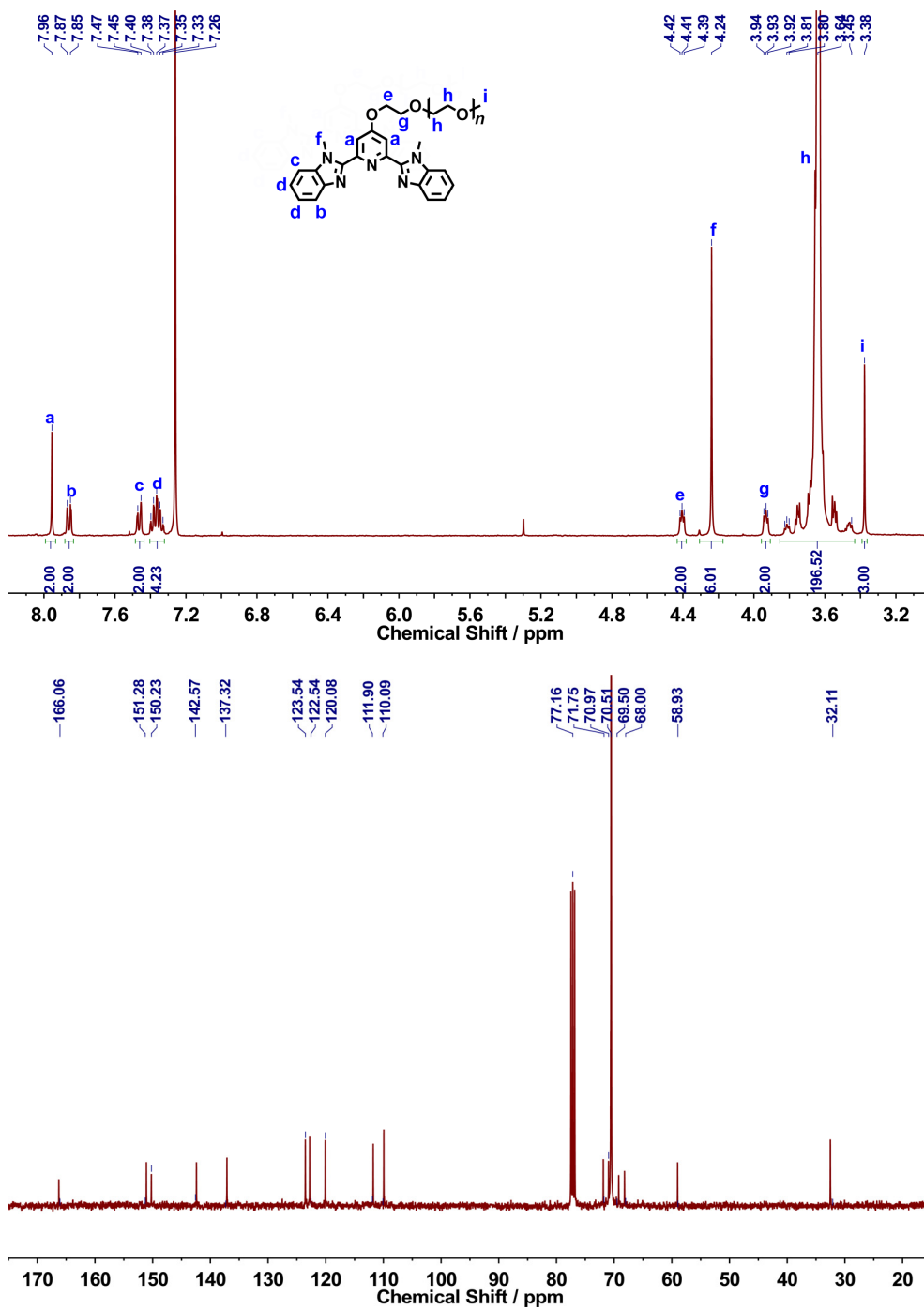
Fig. S3 ^{1}H (Top) and ^{13}C NMR (Bottom) spectra of **MePEG$_{45}$-L** in CDCl$_3$.
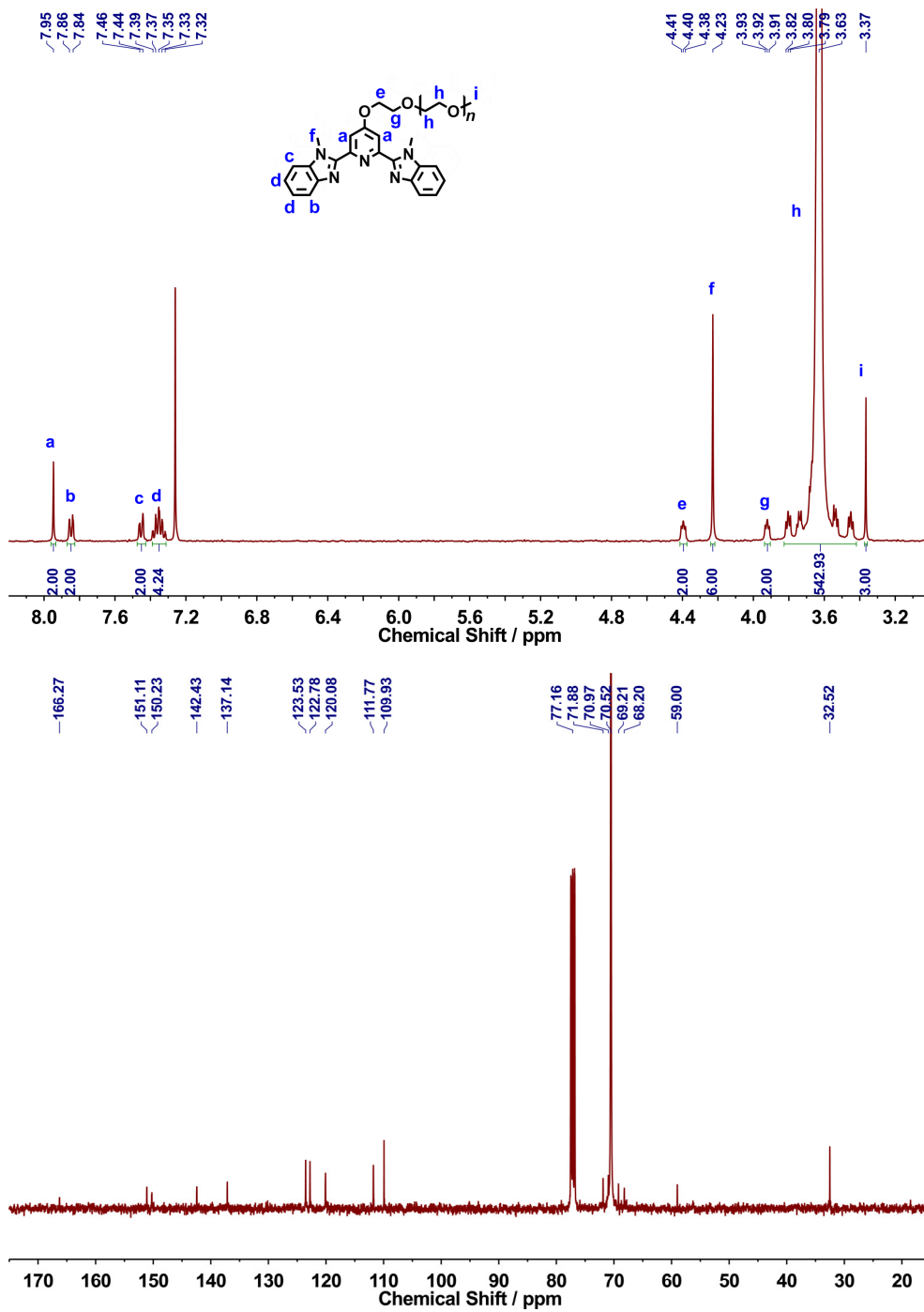
Fig. S4 ^{1}H (Top) and ^{13}C NMR (Bottom) spectra of **MePEG$_{113}$-L** in CDCl$_3$.
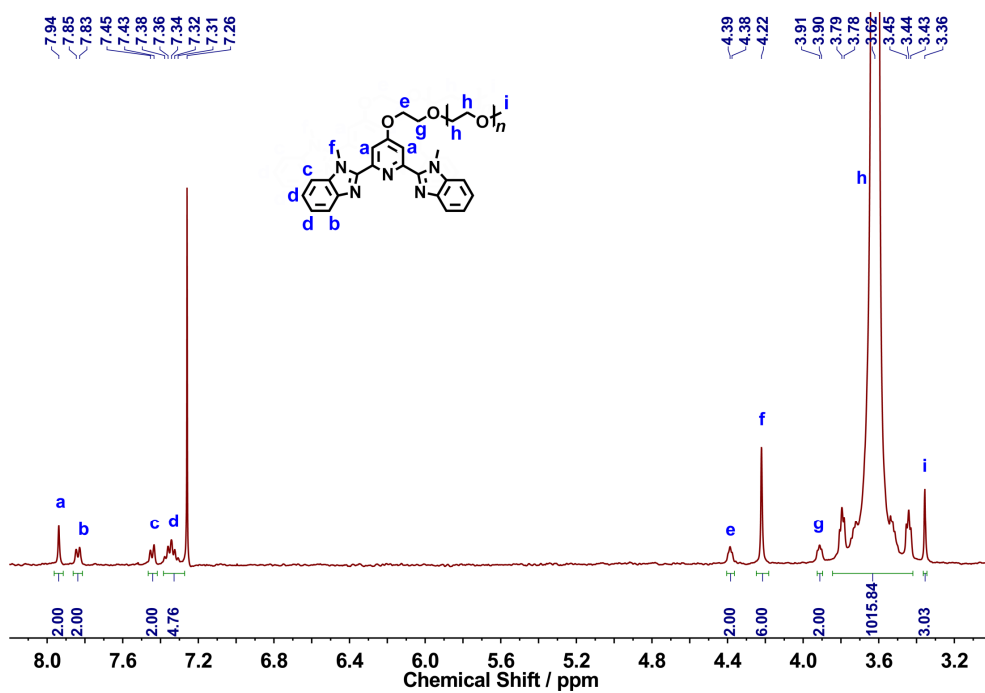
Fig. S5 ^{1}H NMR spectra of **MePEG$_{226}$-L** in CDCl$_3$.
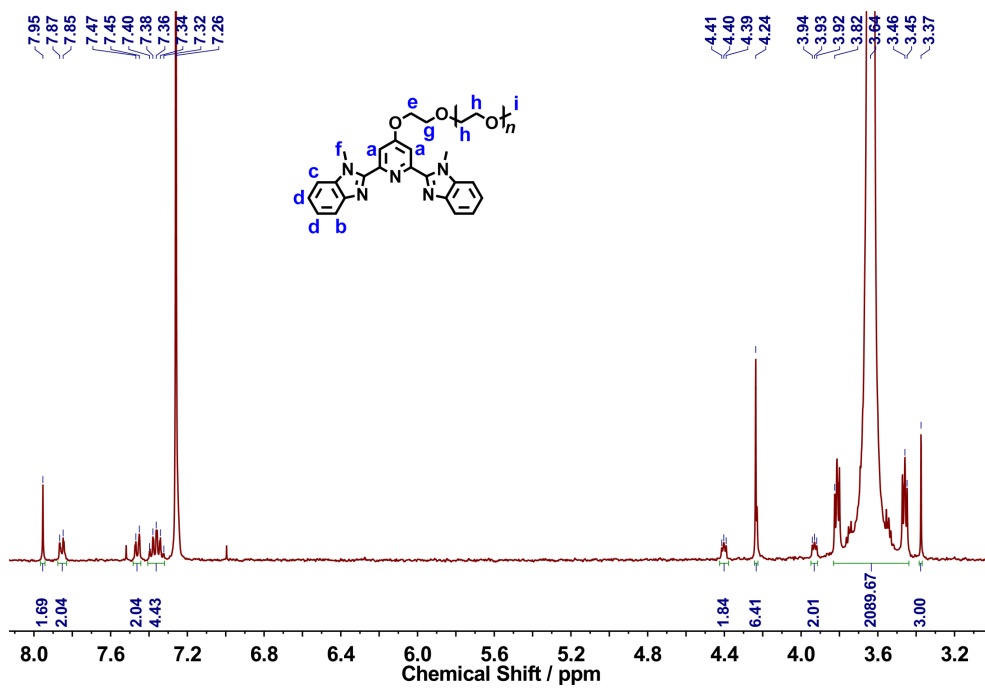
Fig. S6 ^{1}H NMR spectra of **MePEG$_{454}$-L** in CDCl$_3$.
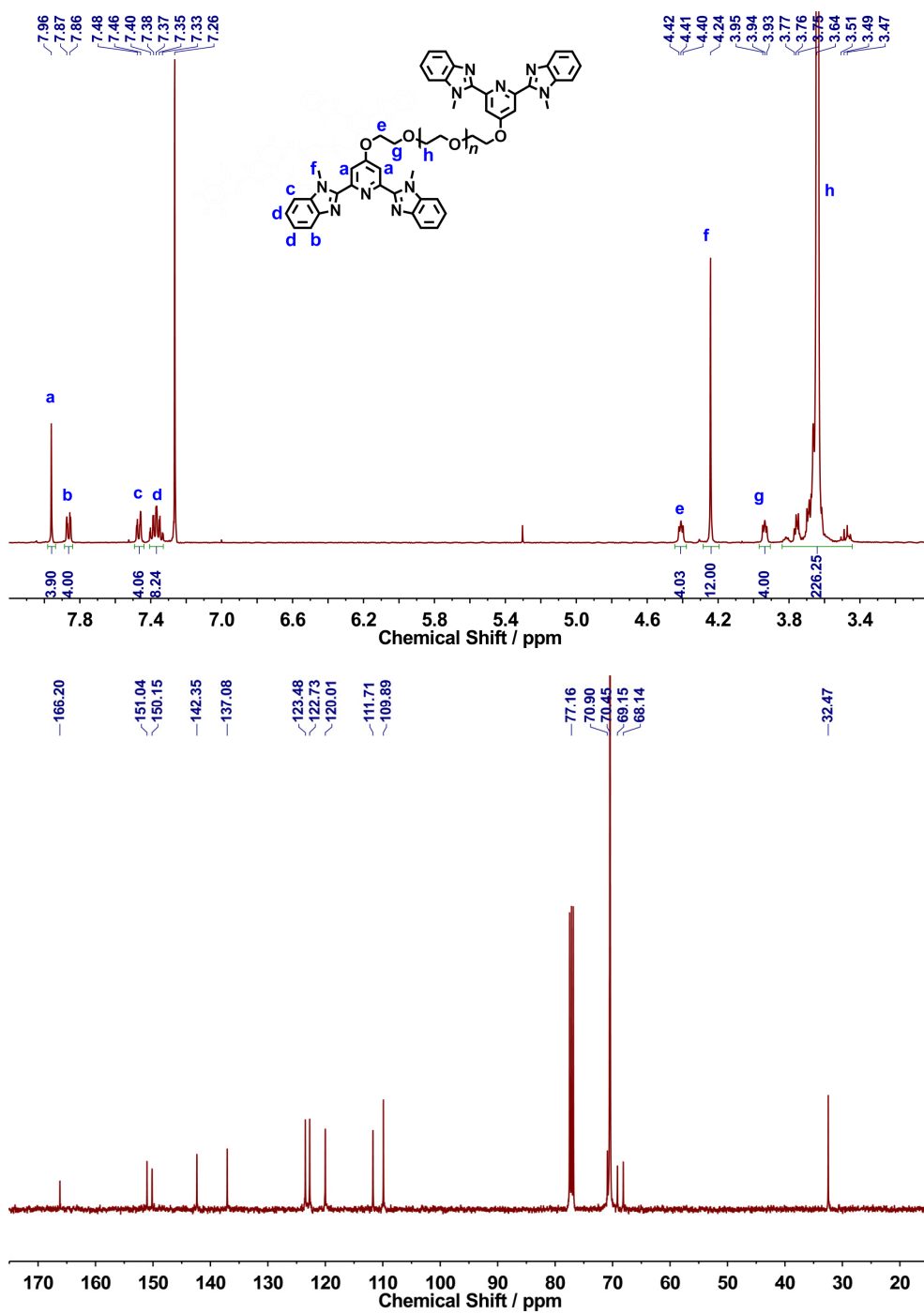
Fig. S7 ^{1}H (Top) and ^{13}C NMR (Bottom) spectra of **MePEG$_{45}$-L$_2$** in CDCl$_3$.
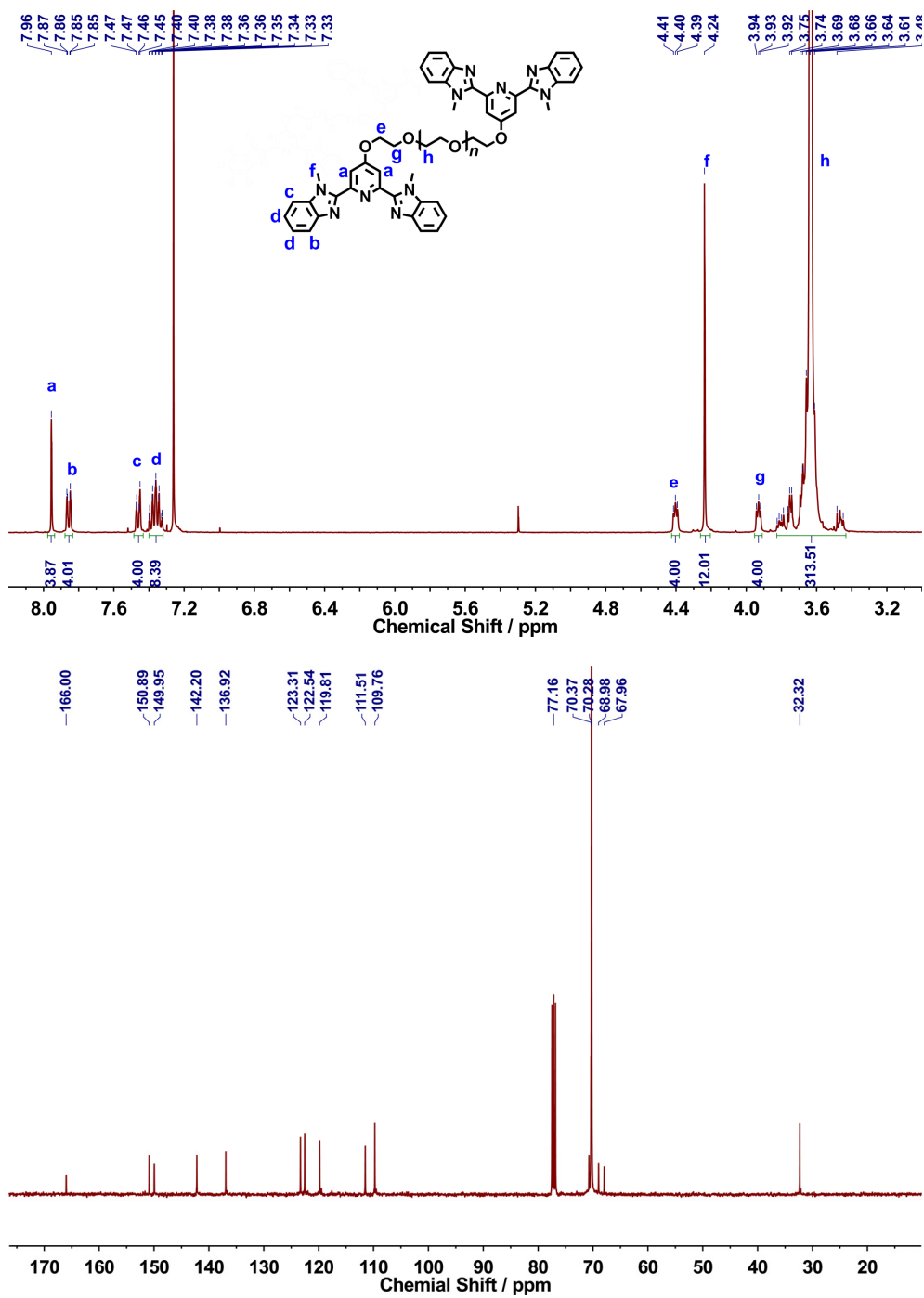
Fig. S8 ^{1}H (Top) and ^{13}C NMR (Bottom) spectra of **MePEG$_{72}$-L$_2$** in CDCl$_3$.
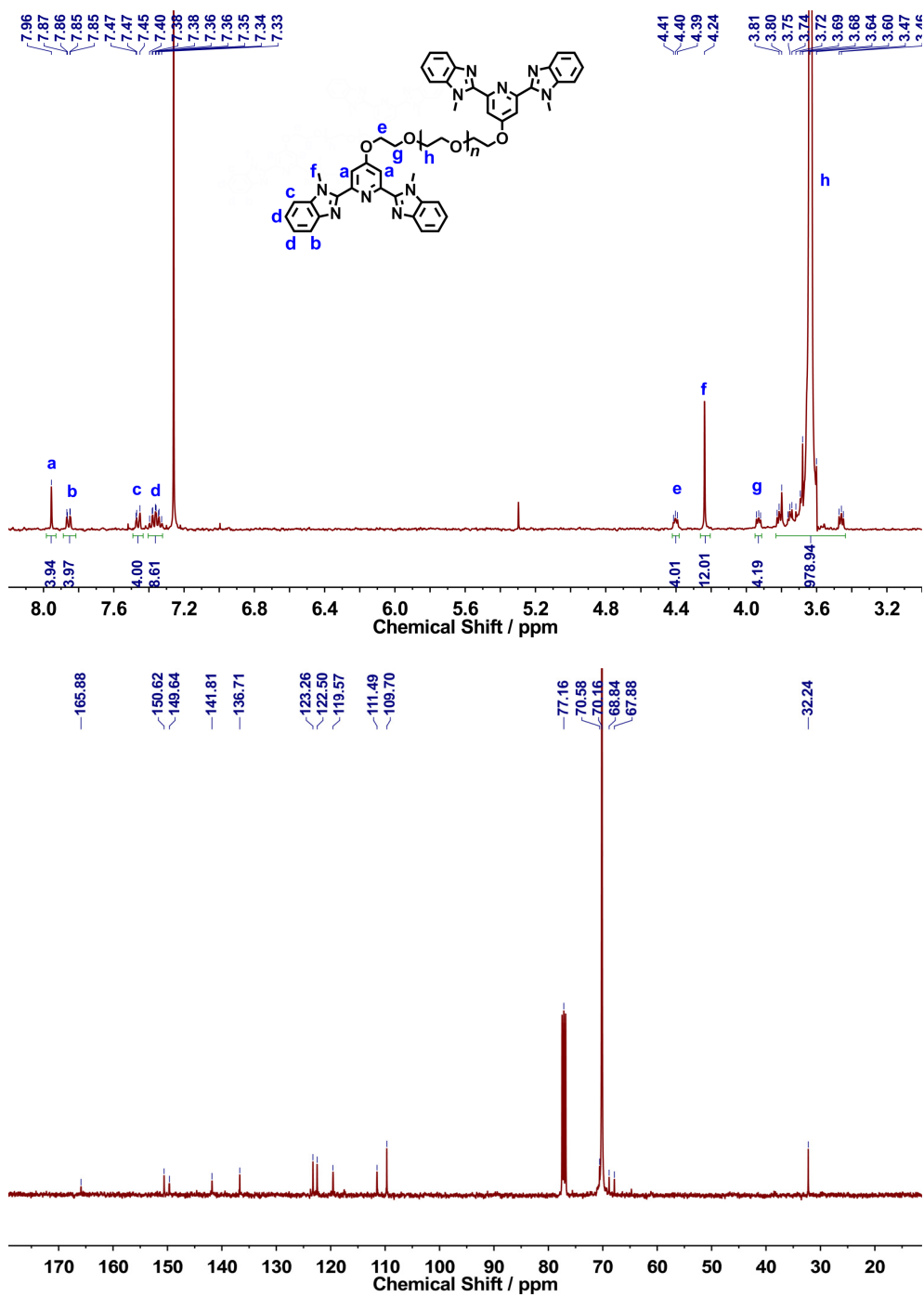
Fig. S9 ^{1}H (Top) and ^{13}C NMR (Bottom) spectra of **MePEG$_{188}$-L$_2$** in CDCl$_3$.

Table S1. GPC Values of PEG End-Functionalized with 2,6-Bis(*N*-methylbenzimidazol-2'-yl) pyridine, MePEG*n*-L and PEG*n*-L$_2$

Sample	M_n / g mol^{-1}	PDI (M_w/M_n)	$M_{n, NMR}$
MePEG$_{45}$-L	2100	1.03	2352
MePEG$_{113}$-L	5100	1.03	5347
MePEG$_{226}$-L	9200	1.04	10325
MePEG$_{454}$-L	21900	1.06	20369
PEG$_{45}$-L$_2$	2400	1.02	2675
PEG$_{72}$-L$_2$	3200	1.02	3864
PEG$_{188}$-L$_2$	9000	1.04	8975

Table S2. Elemental Analyses Established Compositions of Platinum(II)-Containing Metallopolymers

Sample Chemical Formula	Calculated			Found		
	C	H	N	C	H	N
MePEG$_{45}$-Pt $CH_3(OCH_2CH_2)_{45}OC_{21}H_{16}N_5$ $PtCl_2$	51.39	7.66	2.68	49.49	6.63	3.30
MePEG$_{113}$-Pt $CH_3(OCH_2CH_2)_{113}OC_{21}H_{16}N_5$ $PtCl_2$	53.06	8.46	1.25	52.39	8.00	1.25
MePEG$_{226}$-Pt $CH_3(OCH_2CH_2)_{226}OC_{21}H_{16}N_5$ $PtCl_2$	53.75	8.78	0.66	53.21	8.27	0.64
MePEG$_{454}$-Pt $CH_3(OCH_2CH_2)_{454}OC_{21}H_{16}N_5$ $PtCl_2$	54.13	8.96	0.34	53.77	8.38	0.35
PEG$_{45}$-Pt$_2$ $C_{21}H_{16}N_5O_3(OCH_2CH_2)_{45}OC_{21}H_{16}N_5$ Pt_2Cl_4	49.43	6.66	4.37	46.54	5.85	4.81
PEG$_{72}$-Pt$_2$ $C_{21}H_{16}N_5(OCH_2CH_2)_{72}OC_{21}H_{16}N_5$ Pt_2Cl_4	50.81	7.34	3.19	49.03	6.87	3.50
PEG$_{188}$-Pt$_2$ $C_{21}H_{16}N_5(OCH_2CH_2)_{188}OC_{21}H_{16}N_5$ Pt_2Cl_4	52.81	8.31	1.47	52.18	8.37	1.59

Footnote: The macromolecular ligands of **MePEG*n*-L** and **PEG*n*-L$_2$** was completely coordinated to form the platinum(II)-containing polymers of **MePEG*n*-Pt** and **PEG*n*-Pt$_2$**, in which the Pt loading was holden at molar ratios of 1:1 and 1:2 between the polymer ligands and platinum(II) units, respectively. The [Pt(Me$_2$bzimpy)Cl]$^+$ units exhibit luminescence properties, while the PEG chains are non-emissive. Therefore, it is better to use the molecular weights that described the changes in luminescence properties than the Pt loading.
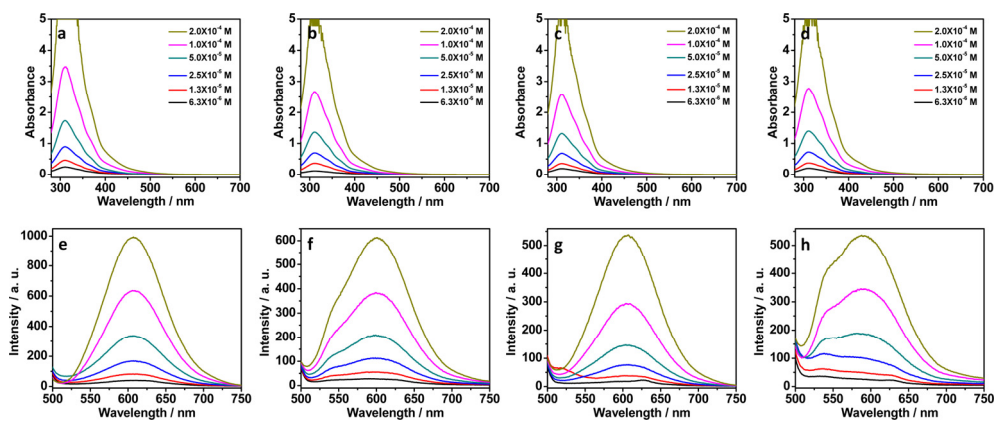
Fig. S10 UV-vis absorption (a-d) and luminescence spectra (e-h) of **MePEG$_n$-Pt** (n = 45, 113, 227, and 454) in water with increasing concentration (6.3×10^{-6}, 1.3×10^{-5}, 2.5×10^{-5}, 5.0×10^{-5}, 1.0×10^{-4}, and 2×10^{-4} mol/L).
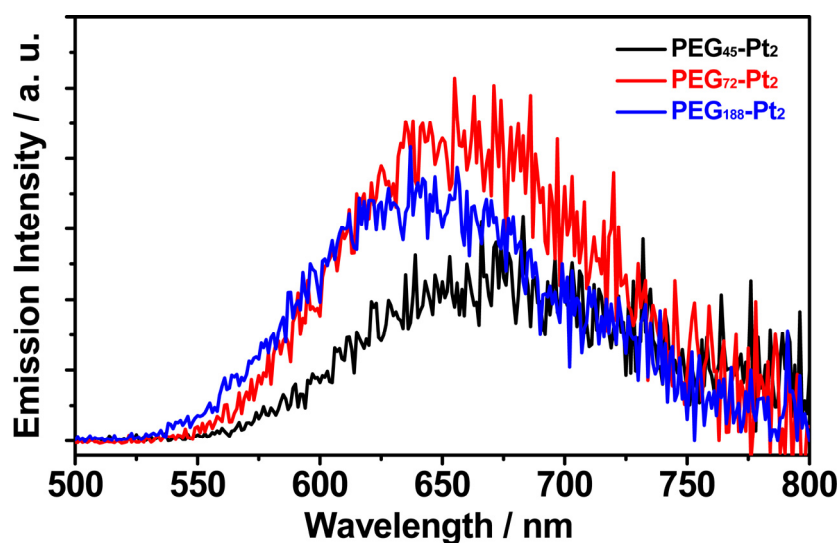

Fig. S11 Emission spectra of **PEG$_n$-Pt$_2$** (n = 45, 72, and 188) in solid states at room temperature (λ_{ex} = 420 nm).
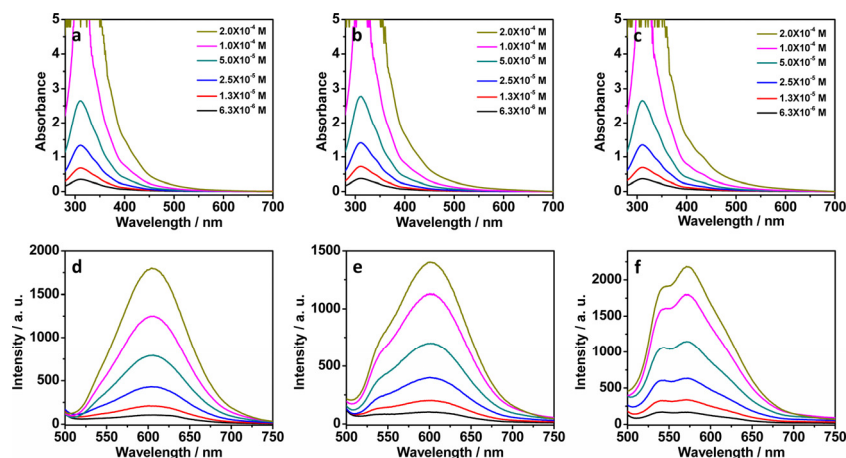

Fig. S12 UV-vis absorption (a-c) and luminescence spectra (d-f) of **PEG$_n$-Pt$_2$** (n = 45, 72, and 188) in water with increasing concentration (6.3×10^{-6}, 1.3×10^{-5}, 2.5×10^{-5}, 5.0×10^{-5}, 1.0×10^{-4}, and 2×10^{-4} mol/L).
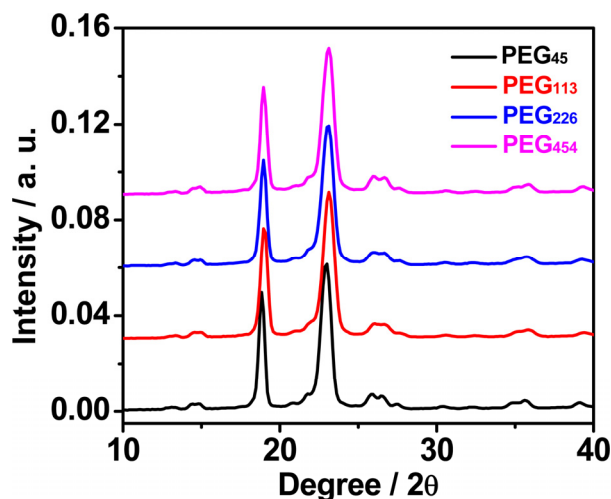
Fig. S13 WAXS data of **PEG$_n$-Pt** (*n* = 45, 113, 227, and 454) in solid states at room temperature.

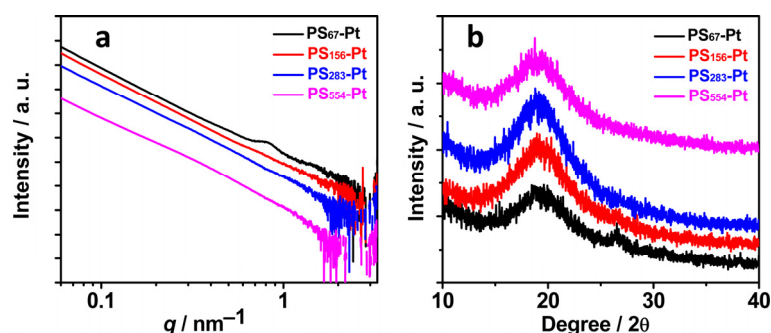**Fig. S14** SAXS (a) and WAXS data (b) of **PS$_n$-Pt** (*n* = 67, 156, 283, and 554) in solid states at room temperature.
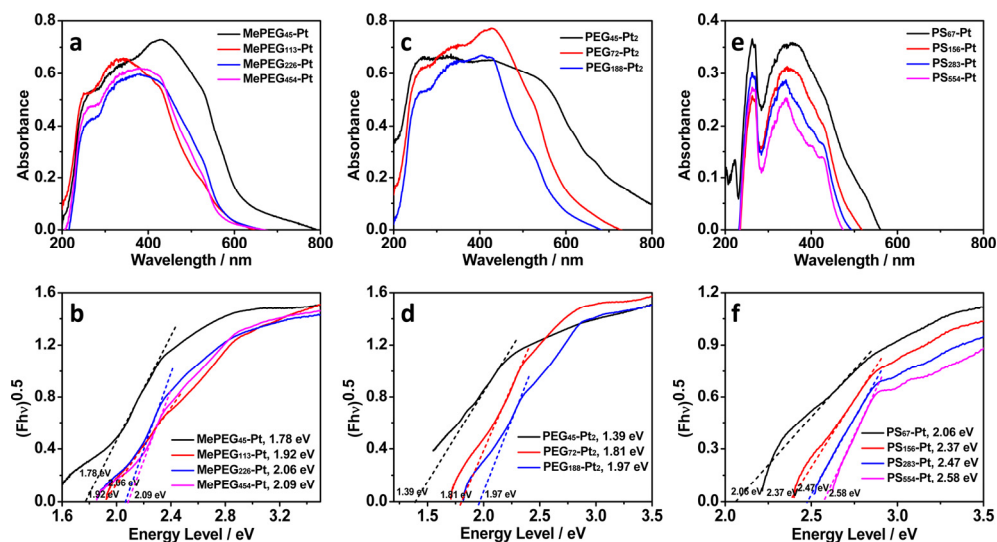

Fig. S15 By increasing the molecular weights of PEGs and polystyrenes, the π–π* band gaps of **MePEG$_n$-Pt** (a and b), **PEG$_n$-Pt$_2$** (c and d), and **PS$_n$-Pt** (e and f) increased, respectively. All of the values of the band gaps were in the range of 0.1-4 eV, indicating typical semiconducting behaviors. The smaller values of the band gaps were demonstrated in the cases of **MePEG$_{45}$-Pt**, **MePEG$_{113}$-Pt**, **PEG$_{45}$-Pt$_2$**, and **PEG$_{72}$-Pt$_2$**, consistent with lamellar morphologies and stronger π–π packing interactions between the platinum(II) planes (See Fig. 2 in the TEXT).

Table S3. The luminescence lifetimes of PEG-based platinum(II) complexes were in the microsecond range, suggesting that the emissions were phosphorescent in nature.

τ / µs		
τ_1 (RW$_1$, %)[a]	τ_2 (RW$_2$, %)[a]	τ_3 (RW$_3$, %)[a]
0.05 (9.13)	0.26 (90.87)	-[b]
0.08 (16.71)	0.28 (83.29)	-[b]
0.13 (19.07)	0.33 (80.93)	-[b]
0.09 (15.37)	0.29 (84.63)	-[b]
0.05 (16.87)	0.17 (62.14)	0.40 (20.99)
0.07 (24.68)	0.21 (65.28)	0.49 (10.05)
0.08 (15.36)	0.24 (55.64)	0.50 (29.00)
0.18 (14.78)	0.56 (65.06)	1.86 (21.16)
0.19 (11.69)	0.61 (63.33)	2.00 (24.97)
0.22 (10.62)	0.67 (58.54)	2.31 (30.84)
0.21 (10.75)	0.67 (62.20)	2.31 (27.25)

[a]Relative weighting (RW) of components in multiple exponential fits. [b]Not detected.

Additional Results and discussion: Both **MePEG$_n$-Pt** and **PEG$_n$-Pt$_2$** were further characterized by UV-vis absorption and luminescence spectra in water. According to previous spectroscopic behaviors of bzimpy-based platinum(II) complexes,[4a,b,S3–S11] intense bands from 280 to 393 nm were attributed to $\pi \rightarrow \pi^*$ transitions of the bzimpy ligands (Figure S10 and S12). Moderately intense metal-to-ligand charge-transfer (MLCT) transitions appeared broadly from 410 to 490 nm (Figure S10 and S12). No additional absorption band was observed in lower-energy regions even at higher concentrations.

Upon excitation at 420 nm for the dilute solutions, weak vibronic-structured emissions appeared at 538 and 572 nm (Figure S10 and S12). The progressional spacings (ca. 1100 cm^{-1}) corresponded to vibrational stretching frequencies of the bzimpy ligands. Therefore, these emissions were assigned to metal-perturbed triplet intraligand charge-transfer excited states of the bzimpy ligands (^{3}ILCT, $\pi \rightarrow \pi^*$). With increasing concentration, the emission bands at 607 nm were remarkably enhanced in the cases of **MePEG$_n$-Pt**, **PEG$_{45}$-Pt$_2$,** and **PEG$_{72}$-Pt$_2$** (Figure S10 and S12), which was accordingly assigned to the excimeric emission that originated from the formation of aggregates with increasing concentration. The driven force was believed to be the π–π stacking interactions between the planar platinum(II) blocks covalently connected with PEGs at higher concentrations. In contrast, in the case of **PEG$_{188}$-Pt$_2$** (Figure S12), no such excimeric emission band was observed, presumably due to larger steric hindrance leading to the absence of the π–π stacking interactions even at higher concentrations.

By fixing one block of diblock copolymers, a continuous increase in the molecular weight of the other block leads to a series of self-assembled nanostructures ranging from micellar to cylindrical to vesicular in solution (Refs. S12*a-d*). The bulk self-assembly generally shows a phase sequence of lamellae, double gyroid, hexagonally packed cylinders, and body-centered cubic-packed spheres (Refs. S12*e-g*). Therefore, the molecular weight is one of key factors to influence the self-assembled nanostructures and their sizes.

In this study, we report the synthesis and luminescence evolution of three sets of platinum(II) complex end-functionalized polymers (MePEG$_n$-Pt, PEG$_n$-Pt$_2$, and PS$_n$-Pt). The emission bands of poly(ethylene glycol)s (PEGs) terminated with platinum(II) complexes (MePEG$_n$-Pt and PEG$_n$-Pt$_2$) were originated from π-π stacking interactions between the platinum(II) planes, which were suddenly blue-shifted with increasing molecular weights of PEGs. Meanwhile, the luminescence quantum yields were found to exhibit a sharp increase. Such dramatic changes are actually originated from the structural transition from lamellar to disordered, and sharply reduced π-π stacking interactions between the platinum(II) planes with the increase in the PEG molecular weights. However, it should be highlighted here that the structuring evolutions from lamellar to disordered have their origins in the molecular weights of PEGs.

MePEG$_{113}$-Pt is monofunctional, while **PEG$_{72}$-Pt$_2$** is a telechelic metallopolymer. The comparison of the luminescence properties is of little significance. They occupy lamellar structures with interlayer spacings of 18.47 and 11.21 nm, respectively. Compared to the higher Φ values of disordered metallopolymers (8.0% for **MePEG$_{226}$-Pt**, 7.4% for **MePEG$_{454}$-Pt**, and 8.5% for **PEG$_{188}$-Pt$_2$**), the Φ values of **MePEG$_{113}$-Pt** and **PEG$_{72}$-Pt$_2$** (2.3% and 3.7%) are at the same level and their difference is only slight and negligible.

References

S1 S. J. Rowan and J. B. Beck, *Faraday Discuss.,* 2005, **128**, 43.

S2 Q. He, H. Huang, X.-Y. Zheng, J. Xiao, B. Yu, X.-J. Kong and W. Bu, *ACS Appl. Mater. Interfaces,* 2018, **10**, 16947.

S3 K. Wang, M. A. Haga, H. Monjushiro, M. Akiba and Y. Sasaki, *Inorg. Chem.,* 2000, **39**, 4022.

S4 L. J. Grove, J. M. Rennekamp, H. Jude and W. B. Connick, *J. Am. Chem. Soc.,* 2004, **126**, 1594.

S5 V. G. Vaidyanathan and B. U. Nair, *Eur. J. Inorg. Chem.,* 2005, 3756.

S6 L. J. Grove, A. G. Oliver, J. A. Krause and W. B. Connick, *Inorg. Chem.,* 2008, **47**, 1408.

S7 I. Mathew and W. F. Sun, *Dalton Trans.,* 2010, **39**, 5885.

S8 C. Po, A.-Y. Y. Tam, K.-M. C. Wong and V.-W. W. Yam, *J. Am. Chem. Soc.,* 2011, **133**, 12136.

S9 N. Liu, B. Wang, W. Liu and W. Bu, *J. Mater. Chem. C,* 2013, **1**, 1130.

S10 J. Liang, X. Zheng, L. He, H. Huang and W. Bu, *Dalton Trans.,* 2014, **43**, 13174.

S11 J. Liang, H. Huang, L. He, N. Liu, Y. Chen and W. Bu, *Dalton Trans.,* 2015, **44**, 66.

S12 (*a*) L. Zhang and A. Eisenberg, *J. Am. Chem. Soc.*, 1996, **118***,* 3168; (*b*) Y.-Y. Won, A. K. Brannan, H. T. Davis and F. S. Bates, *J. Phys. Chem. B*, 2002, **106**, 3354; (*c*) N. J. Warren and S. P. Armes, *J. Am. Chem. Soc.*, 2014, **136**, 10174; (*d*) Y. He, Z. Li, P. Simone and T. P. Lodge, *J. Am. Chem. Soc.*, 2006, **128**, 2745; (*e*) F. S. Bates, *Annu. Rev. Phys. Chem.*, 1990, **41**, 525; (*f*) C. Sinturel, F. S. Bates and M. A. Hillmyer, *ACS Macro Lett.*, 2015, **4**, 1044; (*g*) X.-M. Wang, Y. Shao, P.-F. Jin, W. Jiang, W. Hu, S. Yang, W. Li, J. He, P. Ni and W.-B. Zhang, *Macromolecules*, 2018, **51**, 1110.